EFFECTS OF FRACTURED RESERVOIR ELASTIC PROPERTIES ON AZIMUTHAL AVO

Feng Shen, Xiang Zhu, and M. Nafi Toksöz

Earth Resources Laboratory
Department of Earth, Atmospheric, and Planetary Sciences
Massachusetts Institute of Technology
Cambridge, MA 02139

ABSTRACT

Aligned vertical fractures introduce velocity anisotropy which is directly related to parameters, such as fracture density, fracture shape and fracture contents. Effective medium models allow us to study qP- and qS-wave velocity anisotropy in rocks with aligned vertical fractures, intersecting fracture sets and aligned fractures with small-scale porosity. Spatially varying fracture density distributions result in velocity spatial variations. Stochastic modeling is used to quantify velocity heterogeneity in a fractured reservoir, where the fracture density field is modeled as a stationary Gaussian random field specified by a covariance function describing the amplitude, orientation, characteristic wavenumbers, and roughness of a fracture density field. The goal of the modeling is to relate the stochastic forward model to the statistics of the velocity and seismic reflectivity fields.

Three-dimensional finite difference modeling has been used to investigate the seismic response of fractured reservoirs in P-wave seismic data, and the effects of background Vs/Vp contrasts and anisotropic overburden. The numerical results indicate that background Vs/Vp contrasts across the reflecting boundary, and the presence of anisotropy above the reservoir, have significant effects on azimuthal AVO response at the top of fractured reservoirs. Although a larger Vs/Vp contrast gives rise to a strong AVO response in isotropic media, it is not necessary to give rise to a strong azimuth AVO response. Our numerical modeling shows that the smaller Vs/Vp contrast model gives rise to a strong azimuthal AVO response. Anisotropic overburden always modifies the azimuthal AVO response.

INTRODUCTION

If cracks are spatially aligned in a certain symmetry, the medium is anisotropic. The presence of vertical parallel fractures in a reservoir, which introduces azimuth anisotropy, significantly affects the fluid flow characteristics. Fracture-introduced velocity anisotropy depends on the orientation of individual fracture sets, fracture density, fracture shape, and the bulk modulus of the contained fluids within the fractures. Mueller (1991) used multicomponent shear wave surface seismic data to predict lateral heterogeneity due to variability in fracture intensity in the Austin Chalk. Jordan and Gaherty (1995) formulated stochastic models to specify the small-scale heterogeneity in the anisotropic structure of the continental upper mantle.

Seismic anisotropy induced by aligned fractures has been observed by Crampin and Booth (1985), Crampin *et al.* (1986), Lynn and Thomsen (1990), and Lynn *et al.* (1995). Most data sets indicate that modeling in terms of azimuthal anisotropy is a good approximation. Since P waves are more commonly used than S waves by exploration geophysicists, it is worthwhile to investigate what information regarding azimuthal anisotropy can be extracted from P wave seismic data, and how the properties of the unfractured background rocks affect the seismic response in fractured reservoirs. Although analytical solutions allow for a physical understanding of the relative contributions of anisotropic parameters to the azimuthal AVO response, the application of analytical solutions are limited by the assumption of small impedance contrasts (Rüger and Tsvankin, 1995; Li *et al.*, 1996). 3-D finite difference modeling, however, can handle complicated anisotropic conditions and provide a more complete picture of elastic wave propagation in fractured reservoirs.

In this paper, we study properties of qP and qS-wave velocity anisotropy in three kinds of fractured reservoirs: a single set of vertical fractures, intersecting sets of fractures with different alignments, and fractures with small-scale porosity. Spatial velocity variations from fracture density heterogeneity have been constructed using a 3-D stochastic model. qP and qS-wave velocities are calculated from functional relationships obtained from the effective medium model. 3-D finite difference modeling is used to investigate the effects of background Vs/Vp contrasts and any overlying anisotropy on the seismic response of gas-saturated vertically aligned fractures in a reservoir. The results can be used to guide the interpretation of surface seismic data and fractured reservoir characterization.

THEORETICAL BACKGROUND

Based on average strain concepts (Hill, 1963), Sayers and Kachanov (1995) and Schoenberg and Sayers (1995) presented a method for estimating the effective elastic modulus for fractured media.

$$\epsilon_{ij} = (s^b_{ijkl} + s^f_{ijkl})\sigma_{kl} \tag{1}$$

where ϵ_{ij} is the average strain; s^b_{ijkl} is the compliance tensor of the unfractured background rock; and s^f_{ijkl} is the excess compliance tensor induced by fractures. The excess strain is defined by

$$s^f_{ijkl}\sigma_{kl} = (1/2v)\sum \int_{Sr} ([u_i]n_j + [n_j]u_i)dS \tag{2}$$

where $[u_i]$ and $[u_j]$ are the ith and jth components of the displacement discontinuity on the fracture surface, and n_i and n_j are components of the local unit normal to the surface S.

It is assumed that fracture interactions may be neglected so that $[u_i]$ is determined by σ_{ij}. If all the cracks are aligned with a fixed normal n, the fracture system compliance tensor (Z_{ij}) is introduced with the smoothed linear slip boundary condition.

$$[u_i] = Z_{ij}\sigma_{jk}n_k. \tag{3}$$

Assuming the fracture is invariant with respect to rotation about the axis along the fracture normal direction, the fracture behavior can be described by normal compliance of the fractures (Z_N) and tangential compliance of the fractures (Z_T) (Schoenberg and Sayers, 1995).

$$Z_{ij} = Z_T\delta_{ij} + (Z_N - Z_T)n_in_j, \tag{4}$$

Liu *et al.* (1996) have shown that several different fracture models can be cast into a unified equivalent form. For anisotropy caused by fractures, which are aligned penny-shape cracks, the compliance tensors can be written as follows based on Hudson *et al.* (1996a) and Liu *et al.* (1996).

$$\begin{aligned} Z_T &= (\gamma a^3/\mu)U'_{11} \\ U'_{11} &= U_{11}[1 + \pi/4(\eta/(a/h))^{3/2}U_{11}(3 - 2(Vs/Vp)^2)] \end{aligned} \tag{5}$$

$$\begin{aligned} Z_N &= (\gamma a^3/\mu)U'_{33} \\ U'_{33} &= U_{33}[1 + \pi/4(\eta/(a/h))^{3/2}U_{33}(1 - (Vs/Vp)^2)] \end{aligned} \tag{6}$$

where γ is the number of elementary fractures per area; a is the average radius of a circular shaped crack; η is crack density; U_{11} and U_{33} were given by Hudson (1981). In the Z_N and Z_T expressions, interactions between cracks on a single plane are taken into account through the second terms in the brackets, but interactions between individual

cracks on different planes are neglected. Inserting (3), (4), (5) and (6) into (2), the excess compliance becomes (see Liu *et al.*, 1996).

$$s^f_{ijkl} = \eta/(4\mu)[U'_{11}(\delta_{ik}n_l n_j + \delta_{jk}n_l n_i + \delta_{il}n_k n_j + \delta_{jl}n_k n_i) + 4(U'_{33} - U'_{11})n_i n_j n_k n_l]. \quad (7)$$

The elastic stiffness tensor, from which the seismic velocities can be calculated, is obtained by the inverted compliance tensor.

If multiple fracture sets with different orientations exist and the compliance of one set of fractures depends on the compliance of another, they may not be linearly superimposed. Considering two sets of fractures intersecting each other, the average compliance tensor can be written as:

$$s^b = s^b_0 + s^f_1 \quad (8)$$

$$s = s^b s^f_2 \quad (9)$$

where s^0_b is the compliance tensor of unfractured rock, s^f_1 is the excess compliance tensor as a result of the presence of the first set of aligned fractures, and s^b is the effective elastic compliance tensor of a rock containing the first set of fractures. Similarly, the effective elastic compliance tensor of the fractured system s can be obtained with the new background compliance tensor s^b and the excess compliance tensor s^f_2 induced by the second set of fractures. In this case, s may depend on the order in which fracture sets developed.

The theory above assumes that no porosity exists other than in the aligned fractures. If the background material has small-scale porosity and the pore size is an order of magnitude smaller than the cracks, pressure is relieved within a crack by diffusion into the matrix material rather than by flow through connections to other cracks. Hudson *et al.* (1996b) describe how the existence of connections between otherwise isolated cracks and of small-scale porosity within the 'solid' material affects overall properties of the cracked solid. If the diffusion is linear and normal direction of fractures, only the normal axial stress s gives rise to changes in volume of the cracks, and only the corresponding crack-opening displacement is affected. Following Hudson *et al.* (1996b), the crack-opening displacement is written by:

$$\begin{aligned} U_{33}(p) &= U_{33}/(1+D), \\ \text{where, } U_{33} &= 4/3(\lambda+2\mu)/(\lambda+\mu), \text{and} \\ D &= (1/\pi)(a/c)(\kappa_f/\mu)(\lambda+2\mu)/(\lambda+\mu)/[1+3(1-i)(\omega\phi_m\kappa_f D_m/2)^{1/2}/2c] \end{aligned} \quad (10)$$

where λ and μ are Lamé parameters; a/c is the aspect ratio of a fracture; κ_f is the bulk module; ϕ_m is the porosity; ω is the frequency; and D_m is diffusivity. In this model, the porosity and permeability of the background rock are important parameters affecting $U_{33}(p)$. An isotropic distribution of pores would not have an effect on anisotropy since there is no alignment. However, the effect of fluid diffusion between cracks and the intact background rock on anisotropy should be noted.

PROPERTIES OF VELOCITY ANISOTROPY IN FRACTURED ROCKS

Perfectly Aligned Cracks

For perfectly aligned vertical fractures whose normal is along the horizontal axis (X) in an isotropic background, the medium displays transverse isotropy with a horizontal symmetry axis. Fracture density controls the qP- and qS-wave velocity perturbations, while the fluid contents only affect the normal fracture compliance Z_N, and hence, only the qP-wave velocity (equations (5) and (6)). The decrease of qP-wave velocities in dry (gas-filled) cracked rocks is much larger than those in water-saturated fractured rocks for the same crack density. Moreover, in dry (gas-filled) cracked rocks, P-wave velocity variations are insensitive to crack shape (aspect ratio) and have a dominant $\cos(2\theta)$ variation. In water-saturated cracked rocks, qP-wave velocity variations have a dominant $\cos(4\theta)$ variation for the small aspect ratio and a dominant $\cos(2\theta)$) for the large aspect ratio. Crampin (1986) noted the relationship between the aspect ratio and variation periodicity and he gave a physical explanation: qS-wave velocities are not sensitive to fracture (fluids) contents and have the same velocity values in gas- and fluid-saturated fractures. To demonstrate the qP and qS-wave velocity anisotropy in gas-saturated and water-saturated cracked rocks, we use the Taylor sandstone properties from the table published by Thomsen (1986). The qP- and qS-wave velocities increase from the crack normal direction to the crack strike direction. Numerical results show that qP-wave velocities in gas-saturated fractured sandstone decrease by as much as 38% from 3368 to 2572 m/s with 10% crack density, whereas the qP-wave velocities in water-saturated cracked sandstone only decrease by 5% from 3368 to 3153 m/s for the same crack density. The qS-wave velocity for this example decreases by of 18% from 1828 to 1632 m/s (Figure 1).

Intersecting Cracks

If two sets of nonorthogonal fractures with different fracture densities intersect each other, the elastic stiffness can be calculated according to their development order. After the first set of fractures is inserted, new background effective bulk and shear modulus for the fractured medium can be estimated using the Budiansky and O'Connell's model (1976). By intersecting the second fracture set into the new background effective medium, the effective elastic properties of the rock with two sets of aligned fractures can be estimated by using the scheme described in equations (8) and (9).

To illustrate the effect of intersecting fractures, two sets of gas-saturated fractures, whose alignment directions differ by 30 degrees, are considered in the numerical calculations to show azimuthal velocity anisotropy. The total density is 20%, with the normal of the first set of fractures along the X axis and the normal of the second set of cracks 30°to the X axis. The first set of fractures contains 60% of the total crack density and the second set contains 40%. The horizontal qP- and qS-wave velocity variation

with total crack density is shown in Figure 2a, while the variation with azimuth for the 20% crack density example are shown in Figure 2b. Although the qP-wave velocities vary with azimuth with a dominant $\cos(2\theta)$ periodicity, locations of the maximum and minimum qP-wave velocities are controlled by the combination of the two sets of crack directions and densities. From Figure 2b, it is difficult to detect the individual orientation of each set of fractures. What we can observed is the combined results of two sets of fractures.

Equant Porosity

As mentioned earlier, equant porosity has an effect on the overall properties of fractured rock. From equation (10), it can be shown that equant porosity does not affect qP-wave velocity for gas-saturated fractures. This model is equivalent to the Hudson dry crack model (1981, 1996). In the fluid-saturated case, however, diffusion may have an effect on qP-wave velocity. qP-wave velocities are estimated at seismic frequencies (45 Hz) to show the effects of permeability on water-saturated fractures. Numerical results (Figure 3) show that when permeability is very low, the velocity is similar to that of isolated water-saturated fractures and diffusion is ineffective: when permeability is very high, the velocity is similar to that of gas-saturated cracks, and diffusion has a significant effect on seismic waves. With the same permeability or the same diffusivity, velocity variations are proportional to porosity. Only if the factor Dm is very small, can the equant porosity be ignored from a numerical point of view.

STOCHASTIC MODELING OF FRACTURE HETEROGENEITY

The effective compliance tensor of fractured rock can be written as the sum of the compliance tensor of the unfractured background rock and the excess compliance tensor induced by fractures. The velocity in fractured rock can be decomposed into two parts: the deterministic part (V_0) representing the large-scale heterogeneities, and the stochastic part representing small scale inhomogeneities resulting from fractures.

$$V = V_0 + \delta V. \tag{11}$$

In the previous section, we assumed a statistically homogeneous fracture density distribution. In this section, we study spatial heterogeneity and the processes controlling it. For stochastic modeling to be practical, the fracture density field $\rho_0(x)$ is assumed to be a spatially stationary Gaussian random field. Gaussian processes that are wide-sense stationary are also strict-sense stationary. This statement follows immediately from the fact that a complete characterization for a Gaussian process in terms of its finite-dimensional distribution can be constructed from its second-order characterization. Hence, when this second-order characterization is spatial-invariant, so are all finite-dimensional distributions. Since the mean of the process $\rho_0(x)$ represents the

known component of $\rho_0(x)$, at least conceptually it can always be removed from the process to yield a zero-mean process with the same covariance structure.

$$\rho(x) = \rho_0(x) - m_\rho. \tag{12}$$

Therefore, the essential quantity of interest in analyzing the process $\rho(x)$ is its covariance function.

There are several possible choices for covariance functions: Gaussian, exponential and the von Karman functions. In this paper, our covariance function takes the form of a von Karman function whose properties have been described in detail by Goff and Jordan (1988). The function is given as follows:

$$\begin{aligned} C_{\rho\rho}(x) &= \sigma^2 r^\nu K_\nu(r)/2^{\nu-1}\Gamma(\nu) \\ \text{where, } r(x) &= [x^T Q x]^{1/2}, \text{ and} \\ \sigma^2 &= C_{\rho\rho}(0) \end{aligned} \tag{13}$$

where, $K_\nu(r)$ is a modified Bessel function of order ν, $\Gamma(\nu)$ is a gamma function, σ is an amplitude, and Q is a positive-definite, symmetric matrix whose elements are functions of eigenvalues (wavenumbers) k_1, k_2, and k_3, and spatial orientation (θ, ϕ) in the stochastic field. The power spectrum can been obtained by a 3-D FFT of the autocorrelation function (12a).

$$P(K) = 8\pi^{3/2}\sigma^2\Gamma(\nu + 3/2)/(\Gamma(\nu)(U(k)^2 + 1)^{(\nu+3/2)}. \tag{14}$$

$U(k)$ is the dimensionless norm of k (wavenumber) defined by k and spatial orientation (θ, ϕ) k_1^{-1}, k_2^{-1}, and k_3^{-1} are wavenumbers and are proportional to the correlation lengths. When $k_1 m$ k_2, and k_3 have the same values, heterogeneities in the medium are isotropic. When one of the k values is zero, the 3-D heterogeneities of a random field would be reduced to the case of a two-dimensional random field. The parameter ν represents the rate of fall-off of the spectra after some corner wavenumber. Hence, it characterizes the roughness of the random field. Decreasing parameter ν increases the roughness, with the limiting cases of unity and zero corresponding to a random field with a continuous derivative and one which is "space-filling", respectively (Goff and Jordan, 1988).

PROPERTIES OF VELOCITY HETEROGENEITY IN FRACTURED ROCKS

Realization sections of fracture density from 3-D stochastic modeling in the X=0, Y=0 and Z=0 planes are shown in Figures 4. Based on the functional relationship between the fracture density and qP-wave and qS-wave velocities, we could also map velocity heterogeneities stochastically. As mentioned earlier, fractures have no effect on qP-wave and qS-wave velocities in the fracture strike plane and have maximum effect on qP-wave and qS-wave velocities in the fracture normal plane. Differences of velocities in these two

directions can be used to measure velocity anisotropy. For statistically homogeneous-aligned fractures, velocity anisotropy is spatially uniform. Heterogeneities due to spatial variations of the fracture density could result in spatial variations of velocity anisotropy. Figure 5 shows the qP-wave and qS-wave velocities in fracture normal direction in the section Z=0. The fracture realization for this case is the same as Figure 4c, and parameters for Taylor sandstone are used in the calculation (Table 1). Gas-saturated fractures are assumed. The velocity anisotropy in Figure 5 indicates that heterogeneities of the fracture field would make qP-wave amplitude attributes vary spatially and make the reflectivity of the slow qS-wave differ from that of the fast qS-wave. The fast qS-wave is insensitive to the lateral variation in fracture density since its particle motion is parallel to the fractures. The slow qS-wave possesses particle motion perpendicular to the fracture planes, thus variation in lateral fracture density will affect velocity and reflectivity. The variations of lateral reflectivity are related to the correlation lengths and amplitudes of the heterogeneities. Although velocity anisotropy at local points is determined by fracture orientation, heterogeneities of velocity anisotropy are controlled by the stochastic parameters listed previously. The characterization of inhomogeneous fractured reservoirs must consider not only the fracture parameters, such as orientation and density, but also the stochastic heterogeneity parameters such as wavenumbers, orientations of heterogeneity, and so on.

EFFECTS ON SEISMIC RESPONSE OF FRACTURED RESERVOIRS FROM 3-D NUMERICAL MODELING

Velocity anisotropy induced by fractures represents the maximum amount of information that can be obtained from seismic data. Angular-dependent reflection coefficients depend on wave speeds on either side of a reflecting boundary. Therefore, the background Vs/Vp contrast is a significant parameter affecting the reflected amplitudes. If a transversely-isotropic medium with a vertical axis of symmetry (VTI) exists in the rocks overlying a fractured reservoir, a more sophisticated anisotropic model with additional parameters is needed to explain the reflected seismic data. This raises questions such as how the Vs/Vp contrasts and the anisotropic overburden affect reflected amplitudes and how much information about the reservoir velocity anisotropy can be extracted from P-wave seismic data. To answer these questions, we apply 3-D finite difference modeling to compute synthetic seismograms and analyze the P-wave AVO responses in reservoirs with homogeneous aligned fractures. The seismic response of inhomogeneous fractured reservoirs and their azimuthal AVO response will be the topic of a separate paper.

Effect of Background Vs/Vp Contrasts on AVO Signatures

We calculate reflection amplitudes at the interface of two models in which the upper layer is isotropic shale and the lower layer represents the cracked sandstone reservoir.

Background P and S-wave velocities, densities, and fracture parameters are listed in Table 1, from which it can be seen that model 1 has larger Vs/Vp contrast than model 2.

AVO response at the top of a vertically aligned fractured reservoir is expected to change with azimuth. The qP-wave AVO responses calculated from synthetic seismograms in model 1 hardly show any difference in the azimuth 0°(crack normal) plane and the 90°(crack strike) plane at the top of the fractured reservoirs (Figures 6a and 6b). Root mean square amplitudes, estimated from the synthetic seismograms and normalized by that of zero-offset, do not show significant differences in qP-qP AVO effects in two directions. The seismograms from model 2, however, show different qP-qP AVO responses in the two azimuthal directions (0°and 90°) (Figures 6c and 6d), even though the sandstone reservoir in model 2 has the same fracture density as model 1. Normalized root mean square amplitudes from 0°, 45°to 90°show a reduced amount of variations with $\cos(2\theta)$ periodicity within 30°incident angles. AVO gradients decrease as the azimuth changes from 0°to 90°.

Koefoed (1955) shows that the reflectivity of plane longitudinal waves incident at oblique angles on boundaries is strongly affected by the values of the Poisson's ratios of two media. Shuey (1985) derived an approximate expression for the reflection coefficient in isotropic media as a function of Vs/Vp. As near normal incidence seismic data provide information about the change in acoustic impedance between adjacent layers, so the farther offset data gives information about the Vs/Vp change across an interface (Wepfer, 1994). Comparing the seismograms in the fracture strike plane from model 1 with those from model 2, we see that model 1 has a stronger AVO response. The different numerical modeling results may be attributed to the difference in Vs/Vp contrasts. If there is an angular dependence of Vs/Vp at the reflecting boundary, AVO data will show variations of Vs/Vp contrasts with azimuth for certain ranges of incident angles. Perturbations on azimuthal velocity contrasts induced by vertically aligned fractures depends on the properties of isotropic background rocks. AVO responses from model 2 differ from those of model 1 and show more significant azimuthal response, which indicates that small background Vs/Vp contrast gives rise to stronger azimuthal P-wave AVO response. This suggests that azimuthal AVO effects can be more easily observed in rocks with small background Vs/Vp contrasts.

Effect of Transversely Isotropic Shale on qP-qP AVO Response

If the upper shale in our model has transverse isotropy with a vertical axis, qP-wave AVO and azimuthal AVO responses at the top of reservoirs would be affected. Five independent elastic coefficients needed to describe the vertical transverse isotropy (C_{11}, C_{33}, C_{44} C_{66}, and C_{13}) can be replaced by vertical velocities Vp_0 and Vs_0, and three dimensionless anisotropic parameters, ϵ, δ, and γ (Thomsen, 1986). The introduced anisotropic parameters in overlying shale changes the contrasts of ϵ, δ, γ, and Vs/Vp across the interface of reflection. Clearly, different AVO responses would show at the interface between the transversely isotropic shale and the fractured reservoir. Anisotropic parameters for the overlying shale are taken from Thomsen (1986); the parameters,

$\epsilon = 0,\ \delta = 10,\ \gamma = 0.145$ for oil shale are used.

To analyze the effects of the transversely-isotropic shale (the variations of ϵ, δ, γ contrasts) on azimuthal AVO responses, we compare the azimuthal AVO responses obtained from isotropic shale with those from transversely-isotropic shale for models 1 and 2. The reflection amplitudes from model 1 are decreased and the amplitudes from model 2 are increased at fixed offsets, which may be attributed to the change of Vs/Vp across the reflection boundary. Moreover, overlying anisotropy has modified the azimuthal AVO effects in both models. Note that the AVO effects are increased from moderate incident angles, which means that effects from overlying anisotropy are more pronounced at larger angles of incidence (Figure 7). This phenomenon can be explained in terms of the anisotropic parameters. For small angles of incidence, the contributions of $\Delta\epsilon$ are small because the plane is not dipping much in the e direction. For larger angles of incidence, the contributions of $\Delta\epsilon$ are sizable because the plane is dipping steeply in $\Delta\epsilon$, and both $\Delta\epsilon$ and $\Delta\delta$ contribute to the overall AVO response (Blangy, 1994). Numerical results imply that qP-wave AVO response in fractured reservoirs is complicated when overlying anisotropy is considered. Overlying anisotropy may always modify the AVO response on the reflecting boundary at nonnormal incidence.

CONCLUSIONS

Azimuthal velocity perturbations and velocity periodicity are controlled by fracture density, fracture orientation, fracture aspect ratio, and fracture contents in media with aligned vertical fractures. If diffusion occurs between the cracks and pores, only qP-wave velocity is affected. Variations of velocity are dominated by diffusivity or permeability, and are also increased with porosity. Small-scale heterogeneity in fracture density could lead to the spatial variation of velocities, which can lead to variations in qP-wave and qS-wave reflectivity. Stochastic parameters would be used to describe the small-scale heterogeneity.

Reflection amplitudes from aligned vertical fractured reservoirs are expected to vary with azimuth. Numerical results indicate that azimuthal AVO responses could be affected by background Vs/Vp contrasts across the reflection boundary. Although the higher background Vs/Vp contrasts across the reflection boundary can give rise to a stronger AVO effect, significant azimuthal AVO response appears in the smaller background Vs/Vp-fractured reservoir model. Overburden anisotropy has an important effect on the azimuthal AVO response due to fractures. Although the azimuthal AVO response is an essential indicator of velocity anisotropy in aligned fractured reservoirs, the qualitative interpretation of crack densities based on the differences of reflection amplitudes in the fracture normal plane and strike plane may not be uniquely made.

ACKNOWLEDGMENTS

We thank Enru Liu of the British Geological Survey for helpful discussions. This work was supported by the Reservoir Delineation Consortium at the Massachusetts Institute of Technology.

REFERENCES

Blangy, J. P., 1994, AVO in transversely isotropic media—An overview, *Geophys., 59,* 775–781.

Budiansky B. and O'Connell R.J., 1976, Elastic moduli of a cracked solid, *International J. of Solid and Structures, 12,* 81–97.

Crampin, S., and D. C. Booth, 1985, Shear-wave polarizations near the North Anatolian Fault: II, interpretation in terms of crack-induced anisotropy, *Geophys. J. R. Astr. Soc., 83,* 75–92.

Crampin, S., Robert McGonigle, and Masataka Ando, 1986, Extensive-dilatancy anisotropy beneath Mount Hood, Oregon and the effect of aspect ratio on seismic velocities through aligned cracks, *J. Geophys. Res., 91,* 12703–12710.

Goff, J. A., and T. H. Jordan, 1988, Stochastic modeling of seafloor-morphology: Inversion of sea beam data for second-order statistics, *J. Geophys. Res., 9*3, 13589–13608.

Hill, R., 1963, Elastic properties of reinforced solids: some theoretical principles, *J. Mech. Phys. Solids, 11,* 357–352.

Hudson, J. A., 1981, Wave speeds and attenuation of elastic waves in material containing cracks, *Geophys. J. Roy. Astr. Soc., 64,* 133–150.

Hudson, J. A., Liu, E., and Crampin, S., 1996a, Transmission properties of a plane fault, *Geophys. J. Int., 125.*

Hudson, J. A., Liu, E., and Crampin, S., 1996b, The mechanical properties of materials with interjected cracks and pores, *Geophys. J. Int., 124,* 105–112.

Jordan, T., Gaherty, J.B., 1995, Stochastic modeling of small-scale anisotropic structures in the continental upper mantle, *Proceedings of the 17th Annual Seismic Research Symposium,* Phillips Laboratory, 433–444.

Koefoed, O. 1955, On the effect of Poisson's ratios of rock strata on the reflection coefficients of plane waves, *Geophys. Prosp., 3,* 381–387.

Li, X. Y., Kuhnel, T., MacBeth, C., 1996, Mixed mode AVO response in fractured media, *66th Ann. Int. Mtg., Soc. Expl. Geophys., Expanded Abstracts,* 1822–1825.

Liu, E., MacBeth, C., Pointer, T., 1996, The effective elastic compliance of fractured rock, *66th Ann. Int. Mtg., Soc. Expl. Geophys., Expanded Abstracts,* 1842–1845.

Lynn, H.B. and Thomsen, L.A., 1990, Reflection shear-wave data collected near the principal axes of azimuthal anisotropy, *Geophysics, 55,* 147–156.

Lynn, H.B., Bates, C.R., Simon, K.M., and van Dok, R. 1995, The effects of azimuthal anisotropy in P-wave 3-D seismic, *65th Ann. Int. Mtg., Soc. Expl. Geophys., Expanded Abstracts,* 727–730.

Rüger, A., and Tsvankin, I. 1995. Azimuthal variation of AVO response for fractured reservoirs, *65th Ann. Int. Mtg., Soc. Expl. Geophys., Expanded Abstracts,* 278–281.

Sayers, C. M., and Kachanov, M., 1995, Microcrack-induced elastic wave anisotropy of brittle rocks, *J. Geophys. Res., 100,* 4149–4156.

Schoenberg M., and Sayers, C. M., 1995, Seismic anisotropy of fractured rock, *Geophysics, 60,* 204–211.

Table 1. Parameters of background rocks and synthetic models for modeling.

	layer	Vp (m/s)	Vs (m/s)	density(g/cm3)	crack density
Model 1	Upper	4358	3048	2.81	
	Lower	3368	1829	2.50	0.10
Model 2	Upper	4500	3000	2.65	
	Lower	4900	3100	2.30	0.10

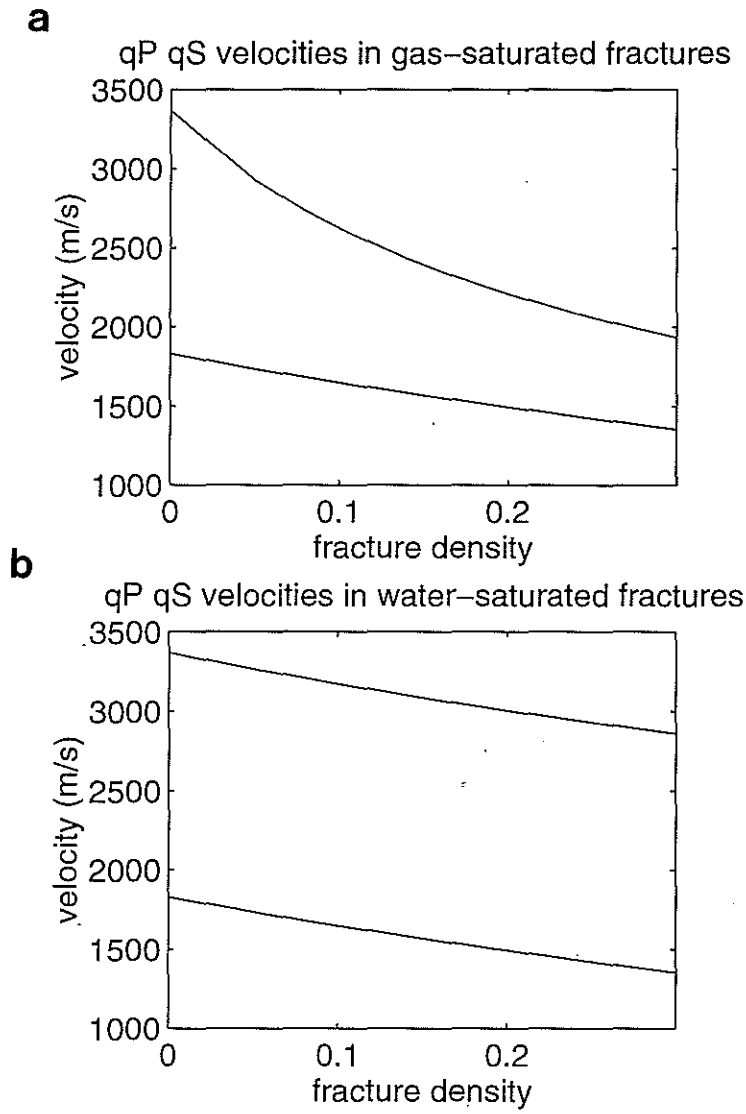

Figure 1: qP-wave and qS-wave velocities as a function of fracture density. (a) Parallel dry (gas-filled) cracks. (b) Parallel water-filled cracks.

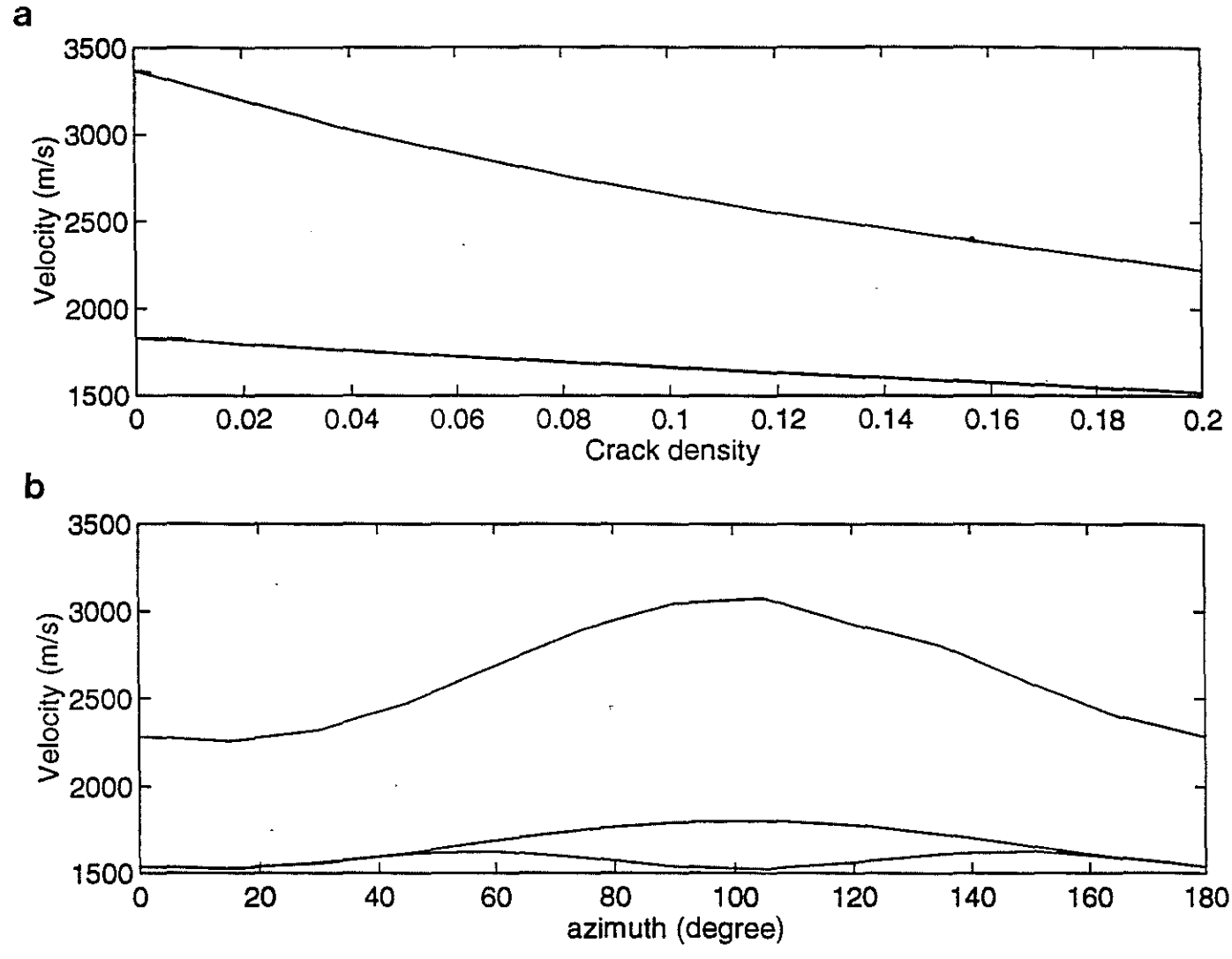

Figure 2: (a) qP-wave and qS-wave velocities as a function of total fracture density for acute intersecting fractures. (b) Variations of qP-wave and qS-wave velocities with angle to the X axis.

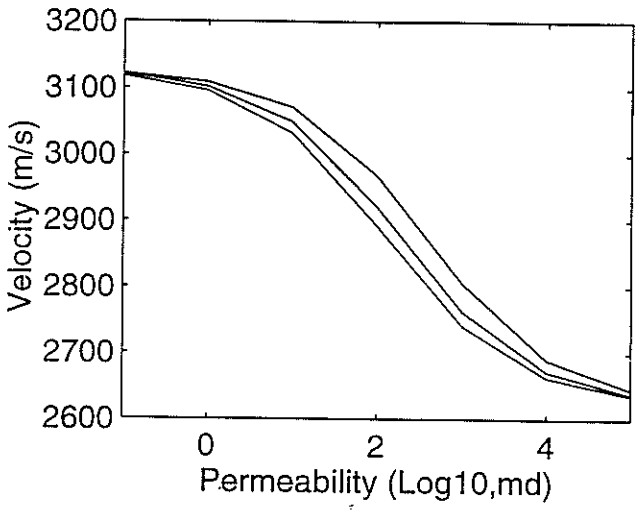

Figure 3: Diffusivity between fractures and pores affects qP-wave velocities. Higher porosity corresponds to larger velocity variations. Curves from the top to the bottom represent porosity 10%, 20% and 30%.

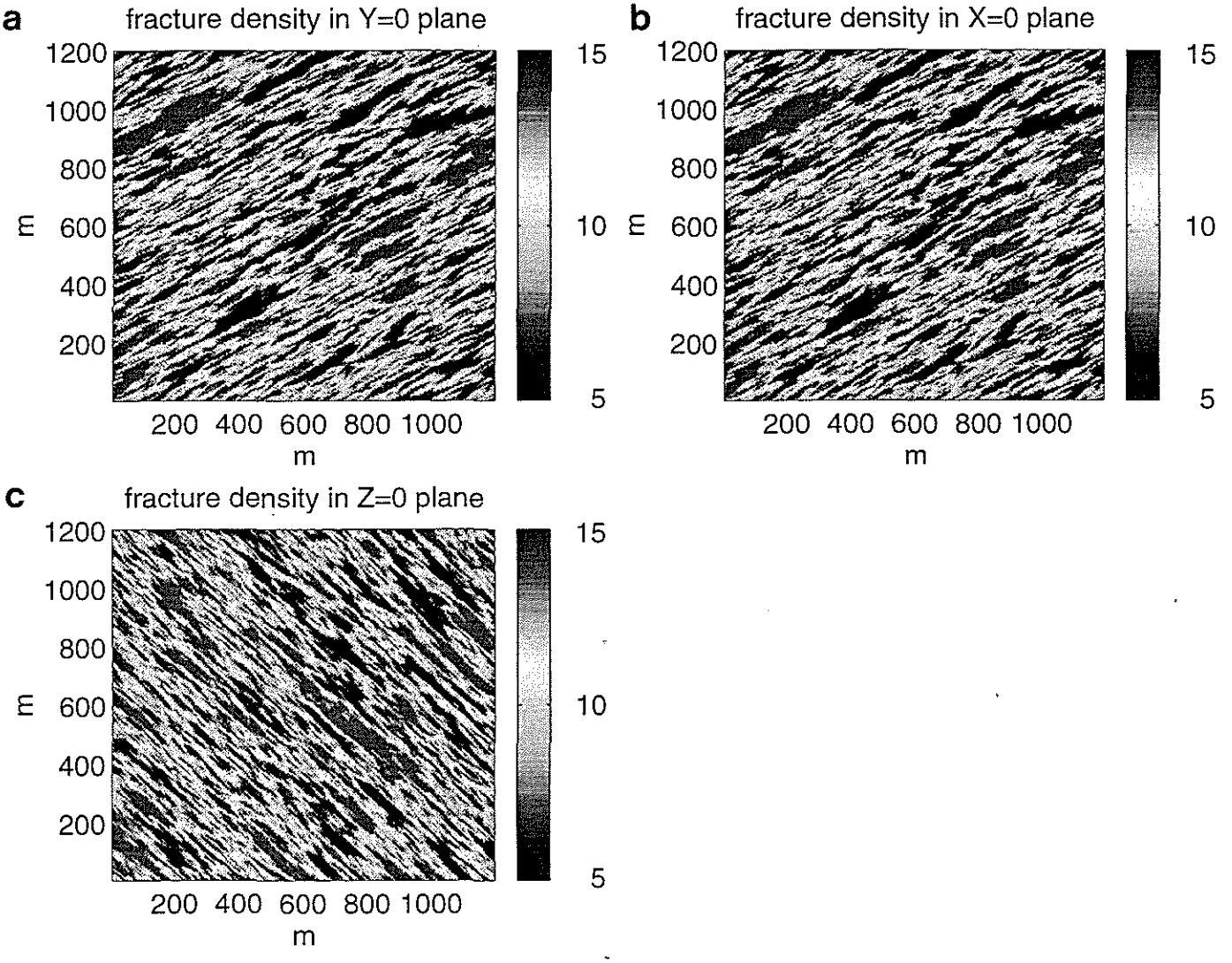

Figure 4: Realizations of fracture density in X=0, Y=0, and Z=0 planes. The wavenumbers are k_x=0.028m^{-1} (0.25 wavelength), k_y=34m^{-1} (0.25 wavelength), k_z=m^{-1} (3.0 wavelength), ν =0.8. The heterogeneity of the fracture field is defined by 60°(θ) and 40°(ϕ). The fracture densities vary between 5% and 15% with mean value 10%.

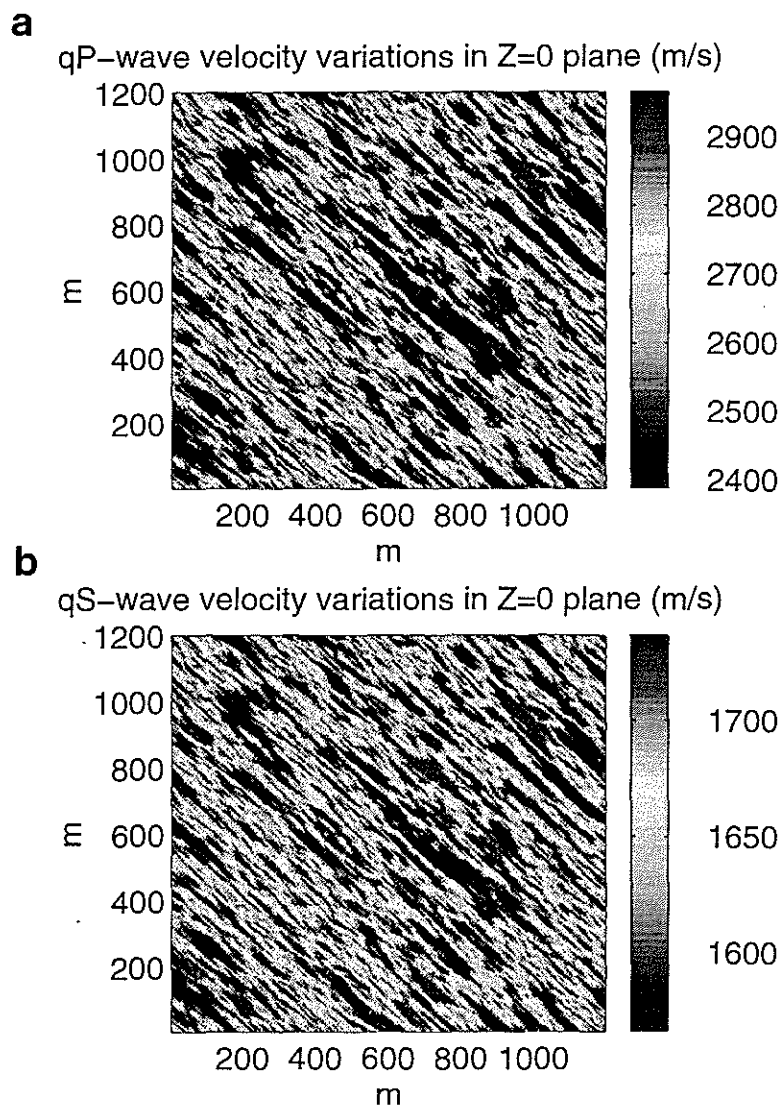

Figure 5: (a) qP-wave velocity heterogeneities in the Z=0 plane. (b) qS-wave velocity heterogeneities in the Z=0 plane.

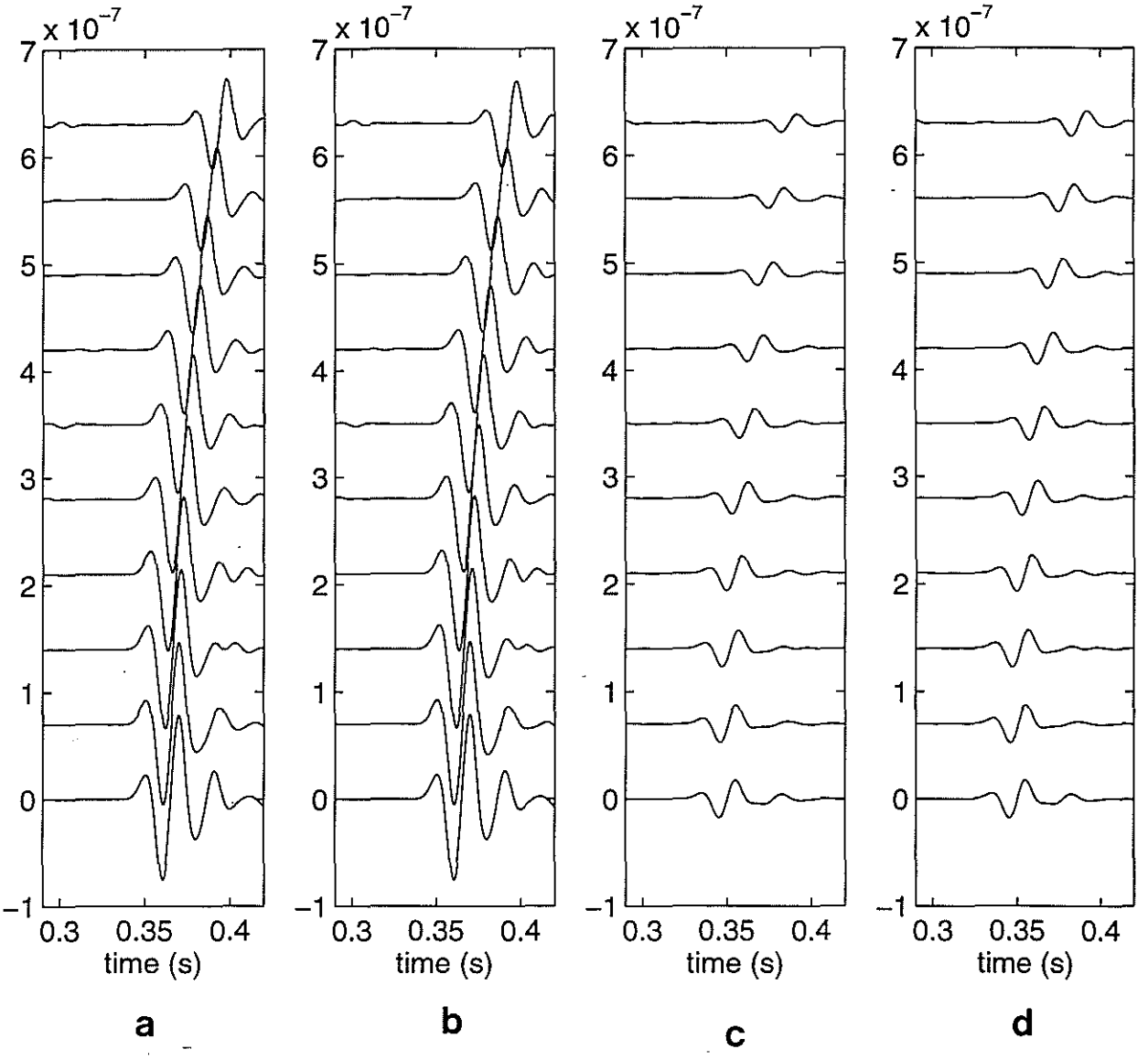

Figure 6: Synthetic seismograms from 3-D finite difference modeling in a fracture normal plane (upper) and a fracture strike plane (lower). (a) Synthetic seismograms in a crack normal plane from model 1. (b) Synthetic seismograms in a crack strike plane from model 1. (c) Synthetic seismograms in a crack normal plane from model 2. (d) Synthetic seismograms in a crack strike plane from model 2.

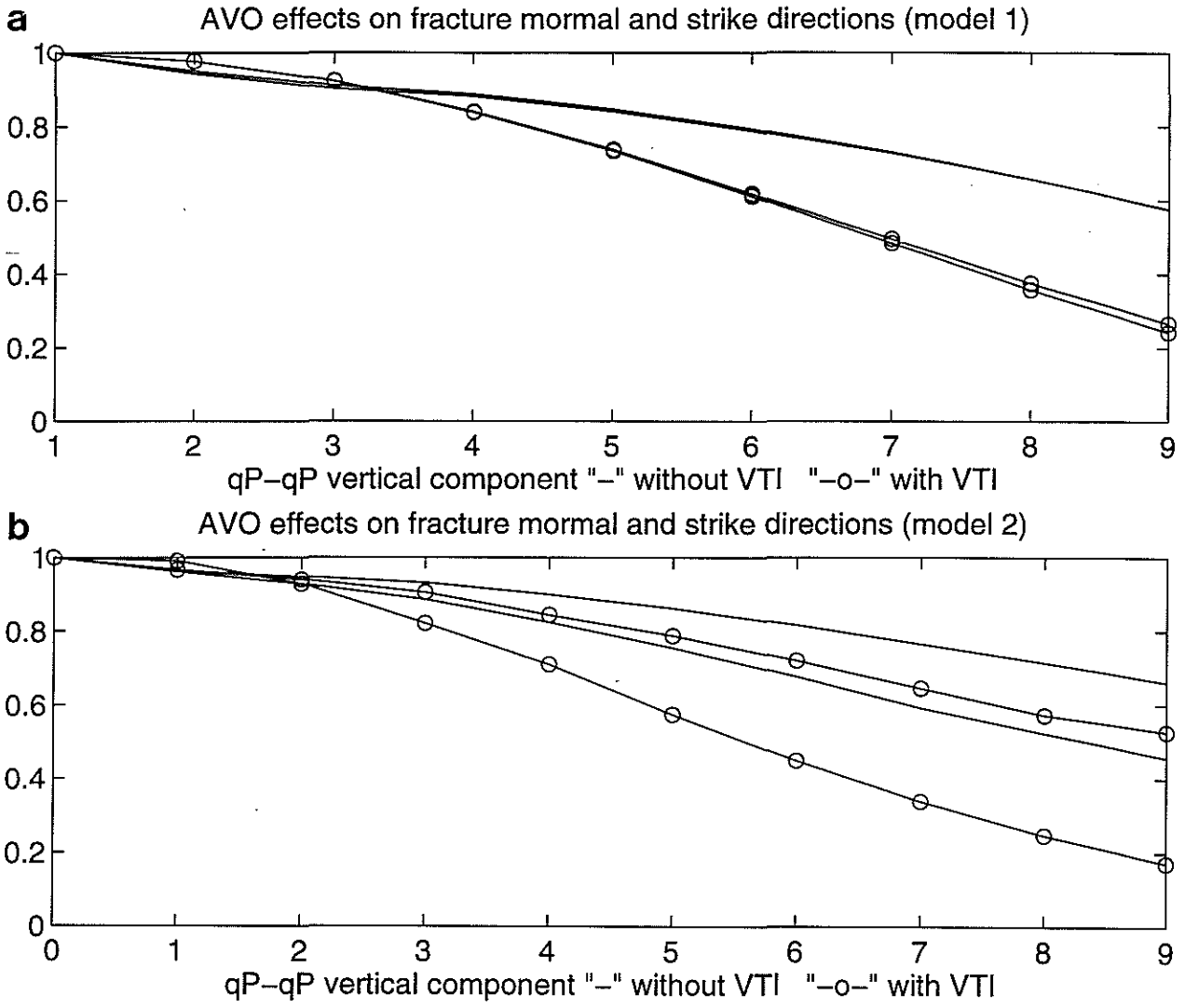

Figure 7: AVO effects from finite difference modeling of model 2 in fracture normal and strike directions. Solid lines with circles represent with effects of overlying anisotropy. (a) AVO from model 1. (b) AVO effects from model 2.